Journal of Power Sources 196 (2011) 8085–8090

Contents lists available at ScienceDirect

Journal of Power Sources

journal homepage: www.elsevier.com/locate/jpowsour

Effect of Y substitution for Nb in $Li_5La_3Nb_2O_{12}$ on Li ion conductivity of garnet-type solid electrolytes

Sumaletha Narayanan, Venkataraman Thangadurai*

Department of Chemistry, The University of Calgary, Calgary, AB T2N 1N4, Canada

ARTICLE INFO

Article history:
Received 5 April 2011
Received in revised form 11 May 2011
Accepted 12 May 2011
Available online 20 May 2011

Keywords:
Metal oxides
Garnets
Li ion electrolytes
$Li_5La_3Nb_{2-x}Y_xO_{12-\delta}$
AC impedance spectroscopy
^{7}Li NMR

ABSTRACT

We report the effect of Y substitution for Nb on Li ion conductivity in the well-known garnet-type $Li_5La_3Nb_2O_{12}$. Garnet-type $Li_5La_3Nb_{2-x}Y_xO_{12-\delta}$ ($0 \le x \le 1$) was prepared by ceramic method using the high purity metal oxides and salts. Powder X-ray diffraction (PXRD), scanning electron microscopy (SEM), ^{7}Li nuclear magnetic resonance (Li NMR) and AC impedance spectroscopy were employed for characterization. PXRD showed formation of single-phase cubic garnet-like structure for x up to 0.25 and above $x = 0.25$ showed impurity in addition to the garnet-type phases. The cubic lattice constant increases with increasing Y content up to $x = 0.25$ in $Li_5La_3Nb_{2-x}Y_xO12-\delta$ and is consistent with expected ionic radius trend. ^{7}Li MAS NMR showed single peak, which could be attributed to fast migration of ions between various sites in the garnet structure, close to chemical shift 0 ppm with respect to solid LiCl and which confirmed that Li ions are distributed at an average octahedral coordination in $Li_5La_3Nb_{2-x}Y_xO_{12-\delta}$. Y-doped compounds showed comparable electrical conductivity to that of the parent compound $Li_5La_3Nb_2O_{12}$. The $x = 0.1$ member of $Li_5La_3Nb_{2-x}Y_xO_{12-\delta}$ showed total (bulk + grain-boundary) ionic conductivity of 1.44×10^{-5} Scm^{-1} at 23 °C in air.

1. Introduction

Nowadays, Li ion batteries are being considered for various ranges of applications, including portable electronics and high power hybrid vehicles due to their high volumetric and gravimetric energy densities compared to that of other known secondary (rechargeable) batteries [1–4]. Constant attempts have been made to replace conventional $LiPF_6$ dissolved organic polyethylene oxide electrolytes in Li ion batteries with inorganic solid electrolytes to overcome the long-term challenges in safety caused by flammable organics, durability due to reaction products at the electrolyte and electrode interfaces, and poor energy density as a result of low electrochemical stability [5–8]. Several solid Li ion electrolytes such as Li_3N, Li-β-alumina, Li_4SiO_4, Li_3PO_4, Li_5MO_4, $Li_{14}ZnGe_4O_{16}$, $Li_{1+x}M_{2-x}M_x^{III}PO_{12}$ (M = Ti, Zr, Ge, Hf; M^{III} = Al, In, Sc), (Li,Ln)TiO_3 (Ln = rare earth) and $Li_5La_3M_2O_{12}$ (M = Nb, Ta) have been investigated [9–11]. Among them, most recently developed garnet-like structured $Li_5La_3M_2O_{12}$ (M = Nb, Ta) and its related compounds show exceptional high Li ion conductivity, and chemical stability with Li metal and high electrochemical stability, which make them as a potential solid Li ion electrolyte for applications in future all-solid-state Li ion batteries [11–13]. The highest total conductivity has been reported for cubic structure $Li_7La_3Zr_2O_{12}$ of about 10^{-4} S cm^{-1} at room temperature [13], while the tetragonal phase showed about two orders of magnitude lower ionic conductivity at room temperature, and comparable value at high temperatures [14].

Following the discovery of garnet-related structured $Li_5La_3M_2O_{12}$, various research have been attempted to improve ionic conductivity by chemical substitution. For examples, substitution of La with the alkaline earth metals resulted the composition of $Li_6ALa_2M_2O_{12}$ (A = Ca, Sr, Ba) and the Ba substituted Ta member showed high ionic conductivity of 4×10^{-5} S cm^{-1} at 22 °C. Also, the Ta members were found to be stable against chemical reaction with molten Li and exhibited high electrochemical stability window of up to ~ 6 V/Li. The structural investigation on the composition $Li_6ALa_2M_2O_{12}$ (M = Sb, Ta) was performed by Cussen and coworkers [15]. In the present study, for the first time, we studied the effect of Y-doping for Nb in $Li_5La_3Nb_2O_{12}$ resulting the composition $Li_5La_3Nb_{2-x}Y_xO_{12-\delta}$ ($0 \le x \le 1$) on the Li ion conductivity with constant lithium ion concentration to understand the role of oxygen defects on transport property. Results obtained from the various solid state techniques, including powder X-ray diffraction (PXRD), ^{7}Li magic angle spinning nuclear magnetic resonance (MAS NMR), and AC impedance spectroscopy are being described.

* Corresponding author. Tel.: +1 403 210 8649; fax: +1 403 289 9488.
E-mail address: vthangad@ucalgary.ca (V. Thangadurai).

0378-7753/$ – see front matter © 2011 Elsevier B.V. All rights reserved.
doi:10.1016/j.jpowsour.2011.05.031

2. Experimental

2.1. Synthesis

The compounds of nominal composition $Li_5La_3Nb_{2-x}Y_xO_{12-\delta}$ ($0 \le x \le 1$) were prepared by a solid-state reaction using appropriate amount of the precursors of high purity $LiNO_3$ (99%, Alfa Aesar) La_2O_3 (99.99%, Alfa Aesar, pre-heated at 800 °C for 24 h), Nb_2O_5 (99.5%, Alfa Aesar) and $Y(NO_3)_3$ (99.9%, Alfa Aesar). $LiNO_3$ was added in 10 wt% excess to account for the loss of Li_2O during annealing. The mixtures were ball milled in Pulverisette, Fritsch, Germany ball mill at 200 rpm for 12 h in 2-propanol using zirconia balls before and after heat treatment at 700 °C for 6 h. The powders obtained were pressed into pellets using isostatic press, (P.O. Weber, Germany) employing a pressure of 300 kN for 5 min. The pellets were sintered at 900 °C for 24 h and 1000–1100 °C for 6 h covered with the same powder to suppress potential volatilization of Li_2O during the preparation. For the chemical stability test, a spinel-type cathode material $Li_2FeMn_3O_8$ was prepared by the conventional solid state method using the high purity precursors such as Li_2CO_3, $FeC_2O_4{\cdot}2H_2O$, and $MnCO_3$ at 700 °C for 24 h in air.

2.2. Characterizations

The pellets were cut into small discs by using diamond wheel (Buehler, Isomet 5000). The phase purity was measured employing powder X-ray diffraction (PXRD; Bruker D8 powder X-ray diffractometer (Cu Kα, 40 kV, 40 mA)). The electrical conductivity of the pellets painted with Au electrodes (cured at 600 °C for 1 h) was measured using Solartron SI 1260 impedance and gain-phase analyzer in the frequency range of 0.01 Hz to 1 MHz in air. The ^{7}Li magic angle spinning nuclear magnetic resonance (MAS NMR) (AMS 300, Bruker) for the powdered samples $Li_5La_3Nb_{2-x}Y_xO_{12-\delta}$ ($x = 0$–0.25) was performed with a spinning frequency of 5 kHz and chemical shift values are expressed against solid LiCl. The morphological studies and elemental analyses were done by scanning electron microscopy (SEM) (Philips FEI XL30). The samples for SEM imaging were in the form of pellets and sputtered with gold on one side and the other side was mounted on the conducting carbon tape. The chemical reactivity test of $Li_5La_3Nb_{1.95}Y_{0.05}O_{11.95}$ with the cathode material $Li_2FeMn_3O_8$ was done by heating 1:1 wt% mixtures at 400, 600, 800 and 900 °C for 24 h in air and resultant product was examined using PXRD.

3. Results and discussion

3.1. Phase characterization

Fig. 1 shows the powder X-ray diffraction (PXRD) patterns of as-prepared $Li_5La_3Nb_{2-x}Y_xO_{12-\delta}$ ($0 \le x \le 1$). A "single-phase" garnet-type structure was observed for x up to 0.25 with very small amount of an unknown impurity peak marked as * in all the compositions. In $x = 0.25$ member, there is an extra peak marked as + which is due to $LiNbO_3$ (Inorganic Crystal Structure Database (ICSD) No. 01-070-8451) and another unknown impurity peak which is marked as x. We could index major peaks on a simple cubic garnet-type structure based on the space group *Ia*−*3d* and is similar to that of the parent compound $Li_5La_3Nb_2O_{12}$ [13]. All the observed lines fit into the cubic phase and there is no evidence for a tetragonal modification, as reported for $Li_7La_3Zr_2O_{12}$ [14]. Table 1 lists the typical indexed PXRD patterns of $Li_5La_3Nb_{2-x}Y_xO_{12-\delta}$ ($x = 0.05$ and 0.1). As anticipated, the cubic lattice constant increases with increasing Y substitution in $Li_5La_3Nb_2O_{12}$ (Table 2) [16]. The six-fold oxygen coordinated Nb (0.64 Å) shows lower ionic radius than that of Y (0.9 Å) [17].

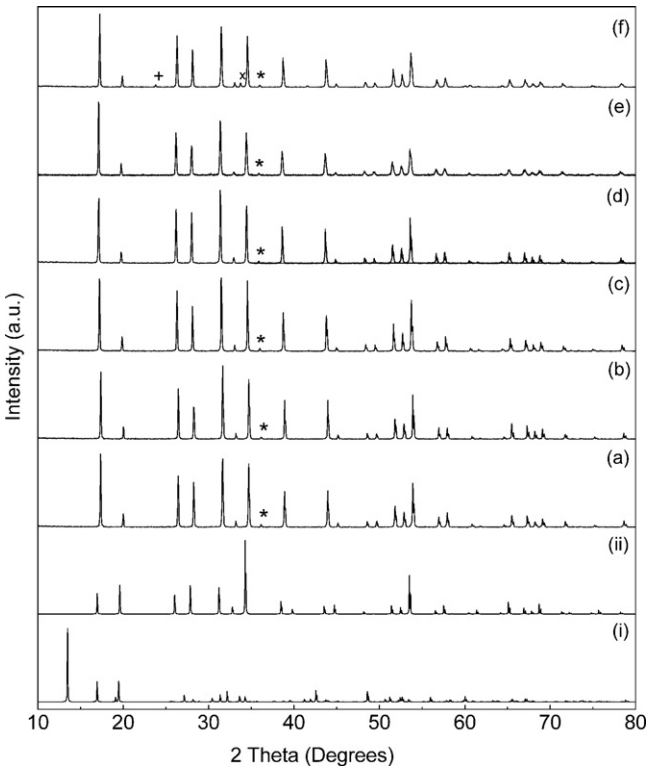

Fig. 1. Powder XRD patterns of $Li_5La_3Nb_{2-x}Y_xO_{12-\delta}$ (a) $x = 0$, (b) $x = 0.05$, (c) $x = 0.10$, (d) $x = 0.15$, (e) $x = 0.20$, and (f) $x = 0.25$. For comparison, the calculated PXRD using PowderCell program of (i) tetragonal $Li_7La_3Zr_2O_{12}$ ($a = 13.130(2)$ Å; $c = 12.675(2)$ Å; space group: $I4_1/acd$) [14] and (ii) cubic $Li_5La_3Nb_2O_{12}$ ($a = 12.80654(11)$ Å; space group: *Ia*−*3d*) [22] are given.

Shown in Fig. 2 are typical SEM images of the as-prepared Y-doped $Li_5La_3Nb_{2-x}Y_xO_{12-\delta}$ and showed that Y substitution influences the particle size. Comparable images were reported for other garnet-type materials reported in the literature [18]. We clearly see that Y substitution for Nb in $Li_5La_3Nb_2O_{12}$ increases the crystallite to crystallite contact. The roughness of the surface seems to happen during sample preparation for SEM using a diamond saw. Based on the SEM study, we could conclude that Y promotes better sintering of the investigated garnet-type materials. The room temperature solid state ^{7}Li magic angle spinning nuclear magnetic resonance (MAS NMR) of $Li_5La_3Nb_{2-x}Y_xO_{12-\delta}$ is presented in Fig. 3. The chemical shift value was expressed with reference to solid LiCl. Very interestingly, all the investigated compounds show a "single peak" at a chemical shift of around 0 ppm and a similar data was reported for several garnet-type structure compound in the literature [19–21]. Accordingly, we believe that Li ion in the investigated compounds may occupy a similar crystallographic site to that of the parent garnet-type $Li_5La_3Nb_2O_{12}$. The narrower the peak may be attributed to fast Li ion mobility in the Y-doped $Li_5La_3Nb_{2-x}Y_xO_{12-\delta}$. It has been proposed that the octahedral site Li ions are more mobile than that of the tetrahedral one and also the occupancy of the former is 2/3 compared to the later which is 1/3 in the parent compound [22–25]. In the present work, the nominal concentration of Li ions was kept constant to elucidate the role of oxygen defects on Li ion conduction. Bond valence analysis showed that the Li ion conduction path seems to be around the transition metal octahedra in the garnet-type framework [26]. However, further experimental studies including neutron diffraction and NMR studies are required to understand the actual crystal structure, chemical substitution reaction, and conduction mechanism.

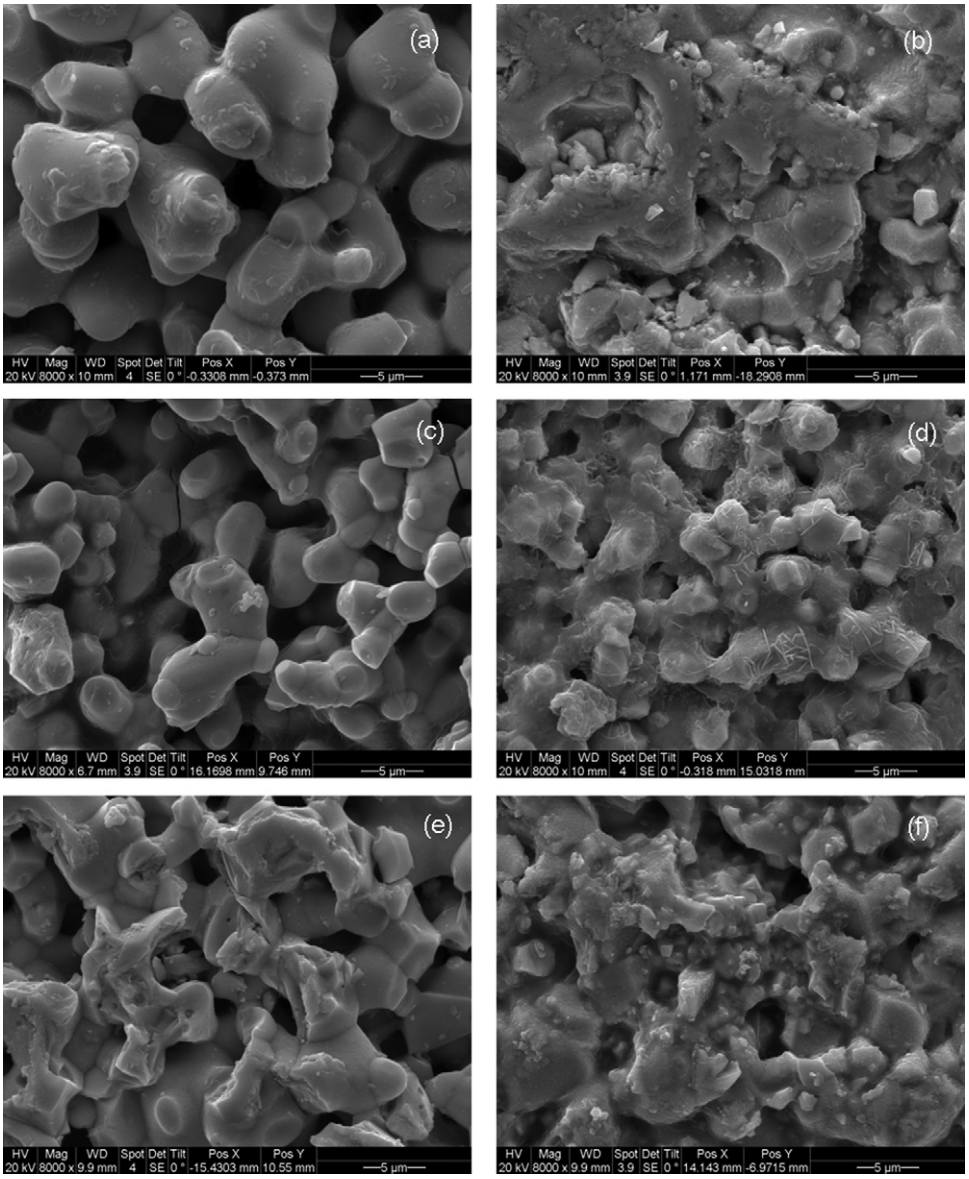

Fig. 2. Typical SEM images of $Li_5La_3Nb_{2-x}Y_xO_{12-\delta}$ prepared at 1100 °C in air (a) $x = 0$, (b) $x = 0.05$, (c) $x = 0.10$, (d) $x = 0.15$, (e) $x = 0.20$, and (f) $x = 0.25$. The Y doping effect on the morphology is clearly seen.

3.2. Electrical properties

AC impedance spectroscopy was used to evaluate the effect of Y doping in $Li_5La_3Nb_2O_{12}$ on Li ion conductivity. Fig. 4 shows typical AC impedance plots of $Li_5La_3Nb_{2-x}Y_xO_{12-\delta}$ at 50 (Fig. 4a) and 150 °C (Fig. 4b). The high frequency portion is zoomed and given as inset figure for clarity. At low temperature, the impedance plots consist of a semicircle and a tail due to the bulk, grain-boundary resistance and electrode effect respectively, at high, intermediate and low frequency regime. While at high temperatures, it becomes more complicated to resolve these contributions meaningfully. Hence, for the calculation of electrical conductivity, the low-frequency side minimum to the real axis was used as resistance '*R*' at low temperatures and the intercept to the real axis was used at high temperatures. A similar approach has been used in the literature to determine the electrical conductivity of garnet-type solid Li ion electrolytes [11–13]. The electrical conductivity was calculated according to the equation:

$$\sigma = \left(\frac{1}{R}\right)\left(\frac{l}{a}\right) \quad (1)$$

where l is the thickness of the sample and a is the area of the electrode. The electrical conductivity as a function of temperature was determined and plotted using the Arrhenius equation:

$$\sigma T = A\exp^{(-E_a/kT)} \quad (2)$$

where A is the pre-exponential term, E_a is the activation energy, T is the temperature, and k is the Boltzmann constant. Fig. 5 shows the Arrhenius plots for electrical conductivity of $Li_5La_3Nb_{2-x}Y_xO_{12-\delta}$ prepared at 1100 °C. The data obtained during the heating and cooling cycle follow the same line, indicated equilibrium behaviour. The substitution of Y for Nb is assumed to create oxygen vacancies in the garnet-type structure for charge compensation. These oxide ion vacancies do not seem to support the Li ion migration in the garnet-type structure. Several authors recently showed the effect of chemical doping such as Sb^V, W^{VI} and Te^{VI} for Nb in $Li_5La_3M_2O_{12}$ (M = Nb, Ta) on the ionic conductivity [27,28]. This approach has decreased the ionic conductivity by several orders of magnitude compared to parent compound because the Li ions occupy the tetrahedral sites, and decrease the concentration of mobile Li ions in the structure. While in the current chemical substitution approach, the

Table 1
Indexed powder XRD patterns of $Li_5La_3Nb_{2-x}Y_xO_{12-\delta}$ ($x = 0.05$; 0.1).

h	k	l	$x = 0.05$			$x = 0.1$		
			$d_{obs.}$ (Å)	$d_{cal.}$ (Å)	$I_{obs.}$ (%)	$d_{obs.}$ (Å)	$d_{cal.}$ (Å)	$I_{obs.}$ (%)
2	1	1	5.093	5.192	100	5.151	5.192	87
2	2	0	4.436	4.496	20	4.469	4.496	22
3	2	1	3.367	3.399	83	3.386	3.399	93
4	0	0	3.156	3.179	53	3.173	3.179	69
4	2	0	2.825	2.844	98	2.838	2.844	100
3	3	2	2.696	2.711	10	2.708	2.711	10
4	2	2	2.583	2.596	98	2.594	2.596	100
5	1	0	2.483	2.494	4	2.493	2.494	5
5	2	1	2.313	2.322	64	2.322	2.322	60
6	1	1	2.059	2.063	64	2.065	2.063	55
6	2	0	2.007	2.011	8	2.015	2.011	6
6	3	1	1.874	1.875	10	1.879	1.875	11
4	4	4	1.835	1.836	9	1.840	1.836	10
6	4	0	1.762	1.764	33	1.768	1.764	42
7	2	1	1.726	1.731	14	1.736	1.731	29
6	4	2	1.700	1.700	73	1.704	1.699	78
6	5	1	1.616	1.615	19	1.621	1.615	15
8	0	0	1.590	1.590	18	1.595	1.590	23
8	2	1	–	–	–	1.526	1.531	5
6	5	3	1.521	1.520	5	1.504	1.520	3
7	5	2	1.443	1.440	4	1.446	1.440	4
8	4	0	1.424	1.422	26	1.428	1.422	20
8	4	2	1.390	1.388	23	1.393	1.388	17
7	6	1	1.374	1.371	14	1.378	1.371	10
6	6	4	1.358	1.356	17	1.362	1.356	14
9	3	2	1.314	1.312	8	1.318	1.312	8
10	1	0	1.263	1.265	4	1.265	1.265	4
10	3	0	1.216	1.218	10	1.219	1.218	10
				$a = 12.717(2)$ Å			$a = 12.717(3)$ Å	

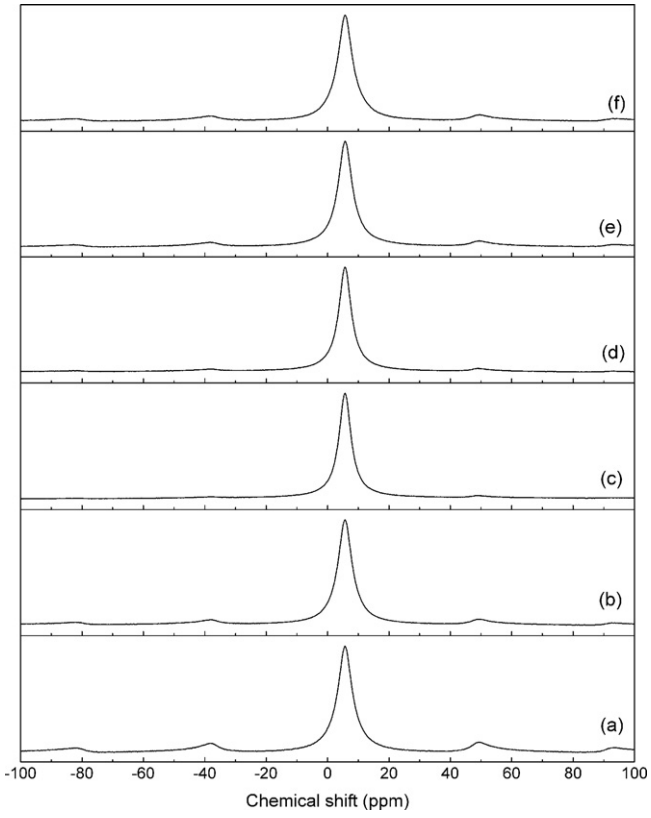

Fig. 3. ^{7}Li MAS NMR of $Li_5La_3Nb_{2-x}Y_xO_{12-\delta}$ sintered at 1100 °C (a) $x = 0$, (b) $x = 0.05$, (c) $x = 0.10$, (d) $x = 0.15$, (e) $x = 0.20$, and (f) $x = 0.25$. The chemical shift values are expressed with respect to solid LiCl.

concentration of Li ions in the investigated compounds is nearly the same; the decrease in the conductivity seems to be attributed to the oxygen vacancy in the structure.

The activation energy for electrical conductivity was found to be in the range 0.5–0.6 eV at 20–200 °C, which is in good agreement with the garnet-type Li ion conductors reported in the literature [11–13]. The electrical conductivity and activation energy of the investigated compounds are listed in Table 2 along with lattice constant. The Li ion diffusion coefficient (D) determined from the AC electrical conductivity using the equation: $\sigma = q^2DN/kT$ (where q is the elementary charge (1.602×10^{-19} C), N is the concentration of Li (could be obtained from the PXRD data), k is the Boltzmann constant (1.38×10^{-23} J K^{-1}) and T is the temperature) was found to be in the order of 10^{-11} to 10^{-12} cm^2 s^{-1} at room temperature and was found to be two orders of magnitude lower than that of other garnet-type materials reported in the literature [18].

In Fig. 6, we compare the electrical conductivity of Y-doped $Li_5La_3Nb_2O_{12}$ with parent $Li_5La_3Nb_2O_{12}$, $Li_6BaLa_2Ta_2O_{12}$, $Li_7La_3Zr_2O_{12}$ and In-doped $Li_5La_3Nb_2O_{12}$ [11–13,18]. We see that Li concentration seems to be important for the electrical conductivity at low temperatures while at high temperatures, all the compounds show comparable ionic conductivity. A slight improvement in conductivity was obtained by the substitution of In for Nb in the structure, which is believed to be due to small change in the Li con-

Table 2
Electrical transport properties of $Li_5La_3Nb_{2-x}Y_xO_{12-\delta}$.

x	Lattice constant (Å)	$\sigma_{(23\,^\circ C)}$ (S cm^{-1})	$\sigma_{(100\,^\circ C)}$ (S cm^{-1})	E_a (eV)
0	12.718(2)	5.08×10^{-6}	5.32×10^{-4}	0.60
0.05	12.717(2)	1.34×10^{-5}	5.94×10^{-4}	0.45
0.10	12.717(3)	1.44×10^{-5}	7.78×10^{-4}	0.51
0.15	12.732(9)	5.71×10^{-6}	1.22×10^{-4}	0.43
0.20	12.743(8)	9.13×10^{-6}	2.70×10^{-4}	0.43
0.25	12.717(5)	9.68×10^{-6}	3.24×10^{-4}	0.43

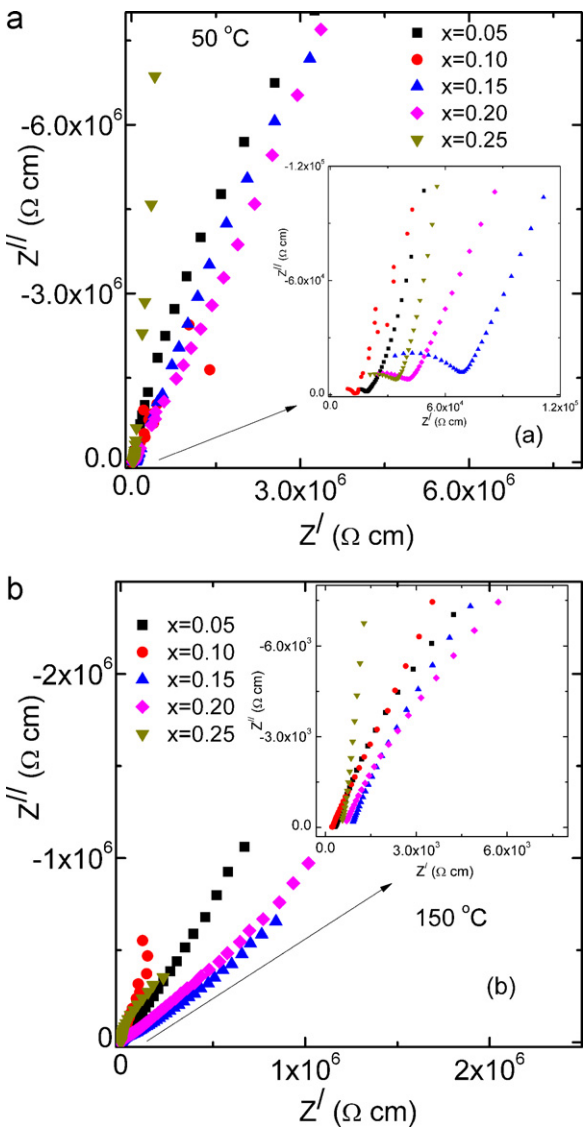

Fig. 4. Typical AC impedance plots in air at (a) 50 °C and (b) 150 °C for of $Li_5La_3Nb_{2-x}Y_xO_{12-\delta}$.

centration and lattice constant. Further increase in the conductivity of about 10^{-5} S cm^{-1} at 22 °C was obtained for $Li_6BaLa_2Ta_2O_{12}$. Recently, the fast Li-ion conducting garnet-related electrolyte with a nominal composition of $Li_7La_3Zr_2O_{12}$ has been reported with a conductivity of 10^{-4} S cm^{-1} at 25 °C. All these results indicate that the increase in Li concentration has a positive effect on the ionic conductivity. The effect of dopant to increase the cell constant and further decreasing the interaction between Li and other ions in the structure can also attributed to the increase in conductivity. The influence of crystal structure on the conductivity is also proved elsewhere [13,14]. For example, Akimoto et al. proved that $Li_7La_3Zr_2O_{12}$ having tetragonal modification was found to show a conductivity about two orders of magnitude lower than that of the cubic phase which is the high ranking garnet-type solid electrolyte for Li ion batteries reported so far [13,14].

3.3. Chemical reactivity

Fig. 7 shows the PXRD patterns of $Li_5La_3Nb_{1.95}Y_{0.05}O_{11.95}$ and the cathode $Li_2FeMn_3O_8$ mixture before heat treatment and after heating at 400, 600, 800 and 900 °C for 24 h. The diffraction patterns clearly indicate the garnet and spinel-type peaks up to 400 °C. After that the garnet-like peaks started disappearing and spinel-type electrode peaks are still present in all the patterns. The new peaks which are clearly seen at 800 and 900 °C could be indexed to $LiLaNb_2O_7$ ($2\theta \sim 28$, 33, 37, 56, 66, and 67°; ICSD No. 00-027-1249) and $LiLa_2NbO_6$ ($2\theta \sim 31$, 45, and 46°; ICSD No. 00-040-0895). These results showed that $Li_5La_3Nb_{1.95}Y_{0.05}O_{11.95}$ is chemically stable with the cathode $Li_2FeMn_3O_8$ up to 400 °C and is promising electrolyte for Li ion battery. Further electrochemical studies need to be done to confirm the range of voltage stability for this particular combination.

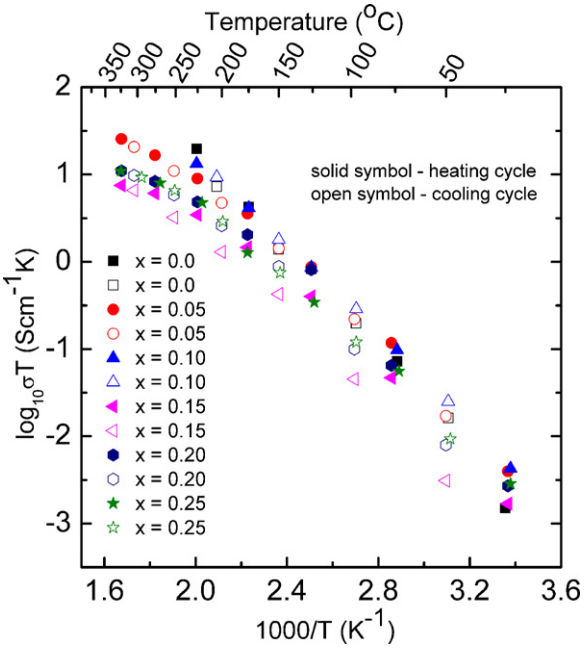

Fig. 5. Arrhenius plots for electrical conductivity of $Li_5La_3Nb_{2-x}Y_xO_{12-\delta}$ sintered at 1100 °C in air.

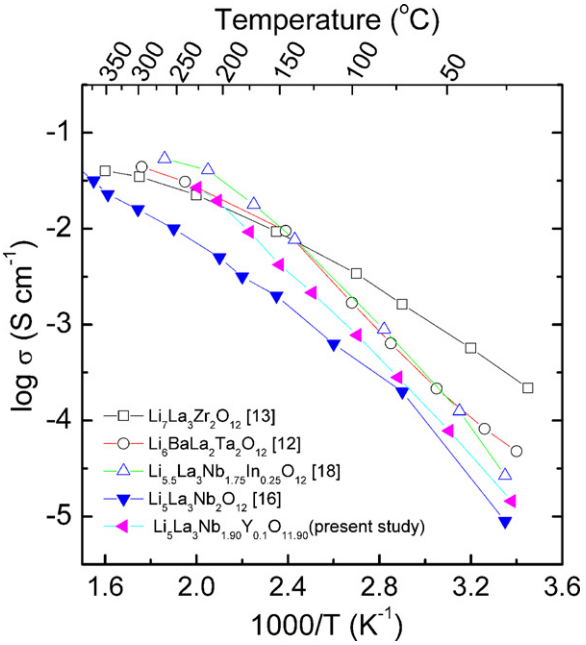

Fig. 6. Comparison of Li ion conductivity of $Li_5La_3Nb_{1.9}Y_{0.1}O_{11.9}$ with other garnet-type solid electrolytes reported in the literature [11–13,18].

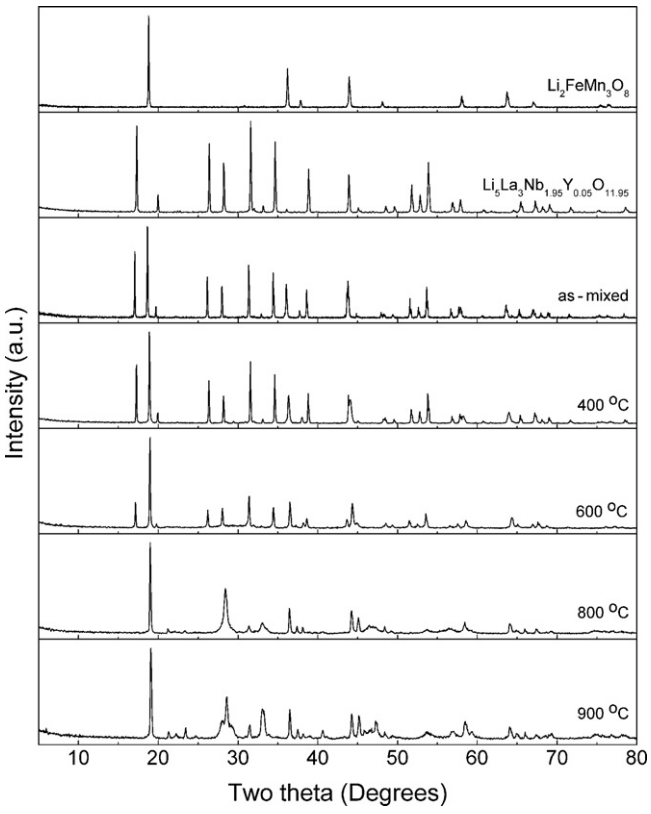

Fig. 7. Powder XRD patterns showing the chemical reactivity between $Li_5La_3Nb_{1.95}Y_{0.05}O_{11.95}$ and $Li_2FeMn_3O_8$ mixture at 400, 600, 800 and 900 °C in air for 24 h. The garnet-like $Li_5La_3Nb_{1.95}Y_{0.05}O_{11.95}$ appears to be chemically stable against reaction with $Li_2FeMn_3O_8$ up to 400 °C.

4. Conclusions

In summary, the present work showed that substitution of Y for Nb in the $Li_5La_3Nb_2O_{12}$ was possible by solid state reaction at elevated temperatures. The powder X-ray diffraction study revealed single-phase cubic garnet-type structure for x up to 0.25 in $Li_5La_3Nb_{2-x}Y_xO_{12-\delta}$ and a very small amount of second phase at high Y doping. AC impedance showed bulk and grain-boundary contribution to the total electrical conductivity and is similar to other garnet-type materials reported in the literature. All the investigated Y-substituted compounds showed comparable electrical conductivity to that of the parent compound $Li_5La_3Nb_2O_{12}$. The $x = 0.05$ and 0.1 members of $Li_5La_3Nb_{2-x}Y_xO_{12-\delta}$ showed ionic conductivity of 1.34×10^{-5} and 1.44×10^{-5} S cm^{-1} respectively at 23 °C, which is about an order of magnitude lower than that of the fast Li ion conducting cubic $Li_7La_3Zr_2O_{12}$. The chemical reactivity of $Li_5La_3Nb_{1.95}Y_{0.05}O_{12-\delta}$ with the cathode $Li_2FeMn_3O_8$ showed that the compound is stable on heating up to 400 °C for 24 h.

Acknowledgement

This research work was supported by the AUTO21 Network of Centres of Excellence, Canada's national automotive research and development program.

References

[1] J.B. Goodenough, Y. Kim, Chem. Mater. 22 (2010) 587–603.
[2] A. Manthiram, J. Phys. Chem. Lett. 2 (2011) 176–184.
[3] B. Scrosati, J. Garche, J. Power Sources 195 (2010) 2419–2430.
[4] J.W. Fergus, J. Power Sources 195 (2010) 939–954.
[5] R.A. Huggins, Elecrrochem. Acta 22 (1977) 773–781.
[6] V. Thangadurai, W. Weppner, Ionics 12 (2006) 81–92.
[7] P. Knauth, Solid State Ionics 180 (2009) 911–916.
[8] G. Adachi, N. Imanaka, H. Aono, Adv. Mater. 8 (1996) 127–135.
[9] S. Stramare, V. Thangadurai, W. Weppner, Chem. Mater. 15 (2003) 3974–3990.
[10] A.D. Robertson, A.R. West, G.A. Ritchie, Solid State Ionics 104 (1997) 1–11.
[11] V. Thangadurai, H. Kaack, W. Weppner, J. Am. Ceram. Soc. 86 (2003) 437–440.
[12] V. Thangadurai, W. Weppner, Adv. Funct. Mater. 15 (2005) 107–112.
[13] R. Murugan, V. Thangadurai, W. Weppner, Angew. Chem. Int. Ed. 46 (2007) 7778–7781.
[14] J. Awaka, N. Kijima, H. Hayakawa, J. Akimoto, J. Solid State Chem. 182 (2009) 2046–2052.
[15] M.P. O'Callaghan, E.J. Cussen, Solid State Sci. 10 (2008) 390–395.
[16] V. Thangadurai, W. Weppner, J. Am. Ceram. Soc. 88 (2005) 411–418.
[17] R.D. Shannon, Acta Crystallogr. A32 (1976) 751–767.
[18] V. Thangadurai, W. Weppner, J. Solid State Chem. 179 (2006) 974–984.
[19] L.V. Wullen, T. Echelmeyer, H.W. Meyer, D. Wilmer, Phys. Chem. Chem. Phys. 9 (2007) 3298–3303.
[20] M.P. O'Callaghan, A. Powell, K. Titman, G. Chen, E.J. Cussen, Chem. Mater. 20 (2008) 2360–2369.
[21] B. Koch, M. Vogel, Solid State Nucl. Magn. Reson. 34 (2008) 37–43.
[22] E.J. Cussen, Chem. Commun. (2006) 412–413.
[23] I.P. Roof, M.D. Smith, E.J. Cussen, H.C. Loye, J. Solid State Chem. 182 (2009) 295–300.
[24] J. Percival, E. Kendrick, P. Slater, Solid State Ionics 179 (2008) 1666–1669.
[25] M.P. O'Callaghan, E.J. Cussen, Chem. Commun. (2007) 2048–2050.
[26] V. Thangadurai, S. Adams, W. Weppner, Chem. Mater. 16 (2004) 2998–3006.
[27] J. Percival, E. Kendrick, P. Slater, Mater. Res. Bull. 43 (2008) 765–770.
[28] E.J. Cussen, T.W.S. Yip, G. O'Neill, M.P. O'Callaghan, J. Solid State Chem. 184 (2011) 470–475.